

PAPER

## Ultra-low noise miniaturized neural amplifier with hardware averaging

To cite this article: Yazan M Dweiri *et al* 2015 *J. Neural Eng.* **12** 046024

### Manuscript version: Accepted Manuscript

Accepted Manuscript is “the version of the article accepted for publication including all changes made as a result of the peer review process, and which may also include the addition to the article by IOP Publishing of a header, an article ID, a cover sheet and/or an ‘Accepted Manuscript’ watermark, but excluding any other editing, typesetting or other changes made by IOP Publishing and/or its licensors”

This Accepted Manuscript is© .

During the embargo period (the 12 month period from the publication of the Version of Record of this article), the Accepted Manuscript is fully protected by copyright and cannot be reused or reposted elsewhere.

As the Version of Record of this article is going to be / has been published on a subscription basis, this Accepted Manuscript will be available for reuse under a CC BY-NC-ND 3.0 licence after the 12 month embargo period.

After the embargo period, everyone is permitted to use copy and redistribute this article for non-commercial purposes only, provided that they adhere to all the terms of the licence <https://creativecommons.org/licenses/by-nc-nd/3.0>

Although reasonable endeavours have been taken to obtain all necessary permissions from third parties to include their copyrighted content within this article, their full citation and copyright line may not be present in this Accepted Manuscript version. Before using any content from this article, please refer to the Version of Record on IOPscience once published for full citation and copyright details, as permissions may be required. All third party content is fully copyright protected, unless specifically stated otherwise in the figure caption in the Version of Record.

View the [article online](#) for updates and enhancements.

# Ultra-Low Noise Miniaturized Neural Amplifier with Hardware Averaging.

Yazan M. Dweiri, Thomas Eggers, Grant McCallum and Dominique M. Durand

**Neural Engineering Center, Department of Biomedical Engineering**

**Case Western Reserve University, Cleveland, OH 44106-4197**

**E-mail addresses: [ymd2@case.edu](mailto:ymd2@case.edu), [tee8@case.edu](mailto:tee8@case.edu), [gam19@case.edu](mailto:gam19@case.edu), [dxd6@case.edu](mailto:dxd6@case.edu)**

*Key words: Electroneurography, high source impedance, nerve cuff electrode, noise reduction, selective neural recording, Parallel Inputs Averaging.*

## **Address Correspondence to:**

Dr. Dominique Durand  
Department of Biomedical Engineering  
Case Western Reserve University  
Cleveland, OH, 44106  
Wickenden 112  
email: [dxd6@case.edu](mailto:dxd6@case.edu)  
phone: 216 368 3974  
fax: 216 368 4872  
web: [nec.cwru.edu](http://nec.cwru.edu)

---

## Abstract

**Objective:** Peripheral nerves carry neural signals that could be used to control hybrid bionic systems. Cuff electrodes provide a robust and stable interface but the recorded signal amplitude is small ( $<3 \mu\text{V}_{\text{RMS}}$  700Hz - 7kHz), thereby requiring a baseline noise of less than  $1 \mu\text{V}_{\text{RMS}}$  for a useful signal-to-noise ratio. Flat Interface Nerve Electrode (FINE) contacts alone generate thermal noise of at least  $0.5 \mu\text{V}_{\text{RMS}}$  therefore the amplifier should add as little noise as possible. Since mainstream neural amplifiers have a baseline noise of  $2 \mu\text{V}_{\text{RMS}}$  or higher, novel designs are required. **Approach:** Here we apply the concept of hardware averaging to nerve recordings obtained with cuff electrodes. An optimization procedure is developed to minimize noise and power simultaneously. The novel design was based on existing neural amplifiers (Intan Technologies, LLC) and is validated with signals obtained from the FINE in chronic dog experiments. **Main Results:** We showed that hardware averaging leads to a reduction in the total recording noise by a factor of  $1/\sqrt{N}$  or less depending on the source resistance. Chronic recording of physiological activity with FINE using the presented design showed significant improvement on the recorded baseline noise with at least 2 parallel operation transconductance amplifiers (OTAs) leading to a 46.1% reduction at  $N=8$ . The functionality of these recordings was quantified by the signal-to-noise ratio improvement and shown to be significant for  $N=3$  or more. The present design was shown to be capable of generating  $<1.5 \mu\text{V}_{\text{RMS}}$  total recording baseline noise when connected to a FINE placed on the sciatic nerve of an awake animal. An algorithm was introduced to find the value of  $N$  that can minimize both the power consumption and the noise in order to design a miniaturized ultralow-noise neural amplifier. **Significance:** These results demonstrate the efficacy of hardware averaging on noise improvement for neural recording with cuff electrodes, and can accommodate the presence of high source impedances that are associated with the miniaturized contacts and the high channel count in electrode arrays. This technique can be adopted for other applications where miniaturized and implantable multichannel acquisition systems with ultra-low noise and low power are required.

## I. INTRODUCTION

There is a growing interest in the field of peripheral nerve interface as an approach to deliver bio electronic medicines [1] and to revolutionize prosthetics. Several studies have been aimed at enhancing the number of extracted voluntary command signals from peripheral nerves over the traditional muscle-driven systems to match the required degrees-of-freedom of advanced robotic arms [2,3, 4]. These approaches include interfacing with cuff electrodes (Spiral [11] and split-cylinder [34]), Interfascicular electrode (slowly penetrating Intrafascicular nerve electrode (SPINE) [5]), intrafascicular electrodes (Longitudinally implanted intrafascicular electrodes (LIFEs) [6], transverse intrafascicular multichannel electrode (TIME) [35]) penetrating electrode (Intraneural Utah Multielectrode Array (MEA)) [7], and regenerative electrodes (Silicon and Polyimide Sieve electrodes) [8]. A particular implementation of the cuff electrode is the flat interface nerve electrode (FINE) [9]. The predefined cross-section the FINE reshapes the nerve to a more flat structure with a larger interface surface, which allows the placement of a larger number of contacts for selective recording of individual fascicle activity within the peripheral nerve trunk. The feasibility of this approach was demonstrated by acquiring two independent signals generated by individual fascicles within intact nerves with a 16-contact FINE [10].

Recording neural activity with nerve cuff electrodes provides several advantages in terms of safety, non-invasiveness and selectivity. However, the neural signals are attenuated by the resistance of the perineurium reducing the magnitude of the detected activity which translates into intrinsically low signal-to-noise ratios (SNR). *In-vivo*, whole-nerve recording studies using single contact cuff electrodes showed that recorded physiological nerve activity has a magnitude range of 0.5 and 3  $\mu V_{RMS}$ . Recording baseline was 0.2 to 0.5  $\mu V_{RMS}$  (2 to 4  $\mu V_{P-P}$ ) with contact impedances up to 1 k $\Omega$  at 1 kHz [11,12].

A limiting factor in minimizing the baseline noise level is the ohmic noise generated by the source resistance. Multiple channel cuff electrodes have high source impedance because of the small contact surface area [13]. Platinum-Iridium contacts with 1  $mm^2$  surface area have an approximate impedance magnitude of 3-6 k $\Omega$  at 1 kHz.

1  
2  
3  
4  
5  
6  
7  
8  
9  
10  
11  
12  
13  
14  
15  
16  
17  
18  
19  
20  
21  
22  
23  
24  
25  
26  
27  
28  
29  
30  
31  
32  
33  
34  
35  
36  
37  
38  
39  
40  
41  
42  
43  
44  
45  
46  
47  
48  
49  
50  
51  
52  
53  
54  
55  
56  
57  
58  
59  
60

Several models have described and quantified the noise generated at the electrode-tissue interface [14]. Nevertheless, assuming that the interface is in redox equilibrium, the noise generated is entirely thermal noise [15]. The range of FINE contact impedances would generate thermal noise between  $0.4 - 0.7 \mu V_{RMS}$  (3 and 5  $\mu V$  pp) which represents the smallest, possible value for the recording baseline. Therefore, the noise added from the acquisition electronics should be minimized in order to keep the recording baseline below  $1 \mu V_{RMS}$  for a useful SNR.

There are two main noise reduction approaches that have been used for neural recording with cuff electrodes. The first technique is power-noise matching by adjusting the optimum noise resistance to match the device's input resistance with an induction transformer [16, 17]. The parameter of interest in this method is the noise figure of the amplifier, which is a practical measure of the degradation of SNR when connected to a non-zero source resistance. It is determined by the ratio of the device-generated noise power to the thermal noise of the source resistance. The best operating condition with the highest SNR will occur when these two noise sources are matched leading to a minimum noise figure. This technique was used in recording neural activity chronically with noise levels as low as  $0.2 \mu V_{RMS}$  using contacts impedance of  $1k\Omega$  [18]. The main drawback of this technique is the size of transformers (the smallest transformer that is currently available is  $8.1 \times 6.7 \times 5.4 \text{ mm}^3$  (EPCOS EP5 SMT pulse transformers series by TDK)). Although this technique was explored for single channel recording, further investigation is needed to study its efficacy for implantable multi-channel recording with the rapidly improving fabrication methods for miniaturized transformers. The second method is noise reduction with averaging parallel input devices (hardware averaging) described in [19]. This method was applied to the measurement of the magnetic field generated by neural activity in peripheral nerves [20], and for evoked neural activity recording (and propagation speed) with longitudinally arranged, multi-contact cuff electrodes [27, 32, 33]. The recorded noise was observed to be reduced by  $(1/\sqrt{n})$ .

Here we apply the concept of hardware averaging to the design of ultra-low noise amplifier to improve the SNR of nerve cuff recordings such as multi-channel FINE. This design has been tested and

validated in chronic recordings of physiological neural activity from the sciatic nerve of a freely moving animal.

## II. METHODS

### A. HARDWARE AVERAGING PRINCIPLE

Neural action potentials generate electrical potential gradients along the nerve surface as they propagate inside the nerve. Detecting these signals requires differential recording between different points along the propagation pathway. Figure 1A shows a demonstration for multi-contact cuff electrode (FINE) and the distribution of the recording points on the nerve. The potential difference between the center contacts (we) and the shorted outer reference contacts (re) is corresponding to the activity generated only inside the cuff. This recording configuration is known as the quasi-tripolar configuration [25, 30].

The most common way to measure this potential gradient is differential recording with instrumentation amplifiers. Any practical instrumentation amplifier generates an intrinsic noise that consists mainly of three components, input voltage noise ( $e_n$ ), current noise at each input terminal ( $i_n$ ), and noise at the output of the amplifier ( $e_{no}$  which is divided by the gain of the input amplifier when referring it to the input).

The electrode-tissue interfaces of the FINE contacts add additional noise sources upon connecting

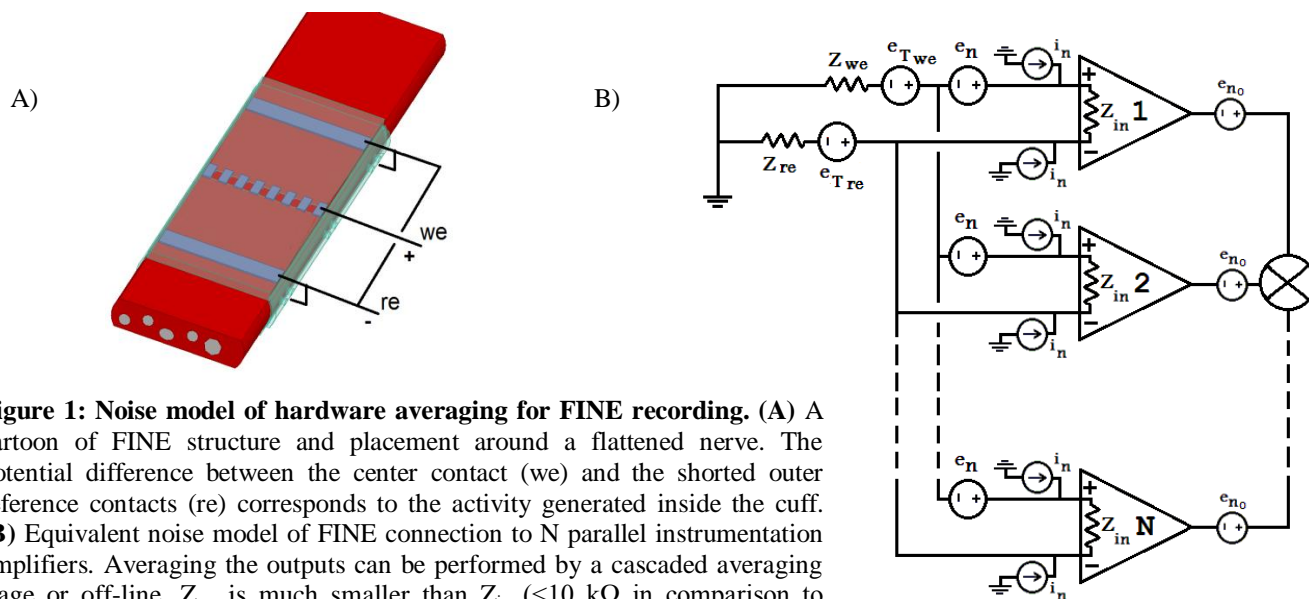


**Figure 1: Noise model of hardware averaging for FINE recording.** (A) A cartoon of FINE structure and placement around a flattened nerve. The potential difference between the center contact (we) and the shorted outer reference contacts (re) corresponds to the activity generated inside the cuff. (B) Equivalent noise model of FINE connection to N parallel instrumentation amplifiers. Averaging the outputs can be performed by a cascaded averaging stage or off-line.  $Z_{we}$  is much smaller than  $Z_{in}$  ( $<10\text{ k}\Omega$  in comparison to  $13\text{M}\Omega$  for the investigated devices), hence the portion of  $i_n$  passing through  $Z_{in}$  is negligible and virtually all of it will pass through  $Z_{we}$  and  $Z_{re}$ .

1 them to the amplifier. This interface noise is usually higher than the thermal noise of the interface  
 2 impedance due to two effects that cause additional voltage fluctuations; first is the random microscopic  
 3 ionic movement at the electrode surface due to irregularities and impurities of the electrode material,  
 4 second is the instability of the fluid film impedance [26]. For the present analysis, it is assumed an  
 5 ideally polarizable electrode with no net Faradic current and the interface is at redox equilibrium,  
 6 therefore the noise generated at the interface are assumed to be purely thermal.  
 7  
 8  
 9  
 10  
 11  
 12  
 13

14 Considering the two types of contacts used in the FINE, the thermal noise generated by the contacts  
 15 equal to  $e_T = \sqrt{4 k T Z}$  and denoted by  $e_{T(we)}$  and  $e_{T(re)}$ .  
 16  
 17  
 18

19 For noise analysis of multiple parallel input devices connected to a FINE (Fig. 2B), the total input  
 20 referred noise is given by (Equation 24 in [21]):  
 21  
 22  
 23

$$V_{n_{IR}} = \sqrt{e_{T(we)}^2 + e_{T(re)}^2 + \frac{1}{N} e_n^2 + N i_n^2 |Z_{re}|^2 + N i_n^2 |Z_{we}|^2 + \frac{1}{N} \left(\frac{e_{no}}{G}\right)^2} \quad (1)$$

24  
 25  
 26  
 27 The conditions for this analysis are: 1) the voltage and current noise sources for each device are  
 28 uncorrelated, 2) the intrinsic noise is random with a mean of zero, and 3) the mean noise power is  
 29 consistent among the parallel devices.  
 30  
 31  
 32

33 Note that the electrodes' thermal noise ( $e_{T(we)}$  and  $e_{T(re)}$ ) and the cumulative current-noise effect

34 ( $\sqrt{N i_n^2 |Z_{re}|^2}$  and  $\sqrt{N i_n^2 |Z_{we}|^2}$ ) are not affected by averaging because they are seen as identical and  
 35 non-random observations (zero variance) among the parallel devices.. However, the input and output  
 36 voltage noise sources ( $e_n$  and  $\frac{e_{no}}{G}$ ) are random among the parallel devices hence they are reduced by  
 37  $1/\sqrt{N}$  upon averaging.  
 38  
 39  
 40  
 41  
 42  
 43  
 44  
 45  
 46

#### 47 *B. IMPLEMENTATION OF HARDWARE AVERAGING FOR NOISE REDUCTION.*

48  
 49 To implement hardware averaging in the design of an ultra-low noise bioamplifier for FINE  
 50 recording, we selected a miniaturized multi-channel CMOS (to ensure low current-noise) amplifier with  
 51 the lowest voltage-noise available. One design that meets this criterion is the OTA amplifier described  
 52 in [22]. This design is commercially available in 32-channel analog and 64-channel fully digitized chips  
 53 (RHA2132 and RHD2164, Intan Technologies, LLC.). These chips have single-ended (unipolar)  
 54  
 55  
 56  
 57  
 58  
 59  
 60

instrumentation amplifiers with one input terminal of each OTA connected to a single common reference input.

The noise performance of the selected CMOS OTA is adequate for most of biopotential recording applications (theoretical  $V_n = 1.7 \mu V_{RMS}$  at 700Hz-7kHz with  $4k\Omega$  source,  $e_n = 20nV/\sqrt{Hz}$ ) but this intrinsic noise is considered high when targeting neural activity of  $1-2 \mu V_{RMS}$  with cuff electrodes.

Starting with the RHA2132 chip, four groups of parallel OTAs were constructed by connecting 8 consecutive OTAs to the same input (Fig.2). The output of each OTA was independently recorded

(32 in total), and then these recorded outputs were averaged off-line in a manner that reflects varying the count of parallel OTAs that is included in the averaging from 1 through 8 OTAs per input.

In order to obtain the current noise for RHA2132 chip, the parameters in Equation (1) were initially isolated with  $Z_{we} = Z_{re} = 0$  to measure  $e_n$ . Then, the current noise impact ( $Ni_n^2|Z|^2$ ) was increased relative to the other terms by connecting a  $200k\Omega$  source resistance ( $Z_{we}$ ) while keeping  $Z_{re} = 0$ . N was varied from 1 through 8 by physically connecting 1 through 8 OTAs in parallel followed by measuring  $V_n$  for each N.  $i_n$  was then calculated by interpolation. These measurements were conducted in a very low-noise environment at a remote location using a portable recording setup.

### C. Data analysis

The OTA outputs were digitized (20kSamples/s) and recorded using the evaluation board and the interface software for the RHA series ship. ENG bandwidth of interest is 700Hz-7kHz and filtering the raw recordings over this bandwidth was performed at two stages; hardware filtering and off-line computational filtering. The hardware filters are internally integrated in the chip (3<sup>rd</sup> order Butterworth

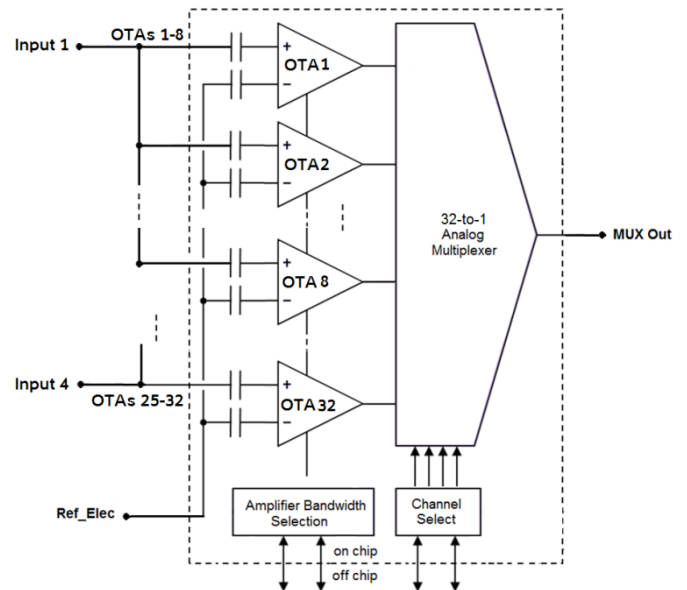


**Figure 2: Schematics of the multi-channel amplifier using hardware averaging.** The averaging technique was applied by connecting the inputs of parallel channels together off-chip, and then average the de-multiplexed outputs of the corresponding channels off-line.

low-pass filter and 1<sup>st</sup> order high-pass filter). Digital filters were applied off-line using MATLAB R2012b software (MathWorks, Inc.).

To quantify the input referred baseline noise, the root mean power of the noise referred to the input is recorded over the ENG bandwidth in  $\mu\text{V}_{\text{RMS}}$ . The noise power density is calculated from the raw signal by applying Fourier transform, then bin-integrated with 200 points (10 ms) window as described in [28].

Statistical tests on the recorded signals are conducted to determine whether or not the means of recording groups are significantly different. These tests consist of one-way ANOVA to determine if there is significant differences within a set of recordings, then post-hoc t-tests is performed to determine with 95% certainty ( $\alpha=0.05$ ) which recording groups are different from which groups. These tests were conducted using Minitab 17 software (Minitab Inc.).

#### D. FINE electrode Fabrication

The FINE was fabricated as two layers of silicon sheet (SSF) enclosing a laser-cut Pt-10%Ir contacts (Part No. 41803 Alfa-Aesar) and fused with a silicon primer (MED-4211 Nusil Silicon Technology). Multi-strand DFT, Teflon-coated wires (1x7x0.001"; Fort Wayne Metals) were spot-welded to the contacts (Fig. 3 A). The exposed area of the center working contacts was 1 mm x 0.5 mm, and for each of the outer reference contacts it was 1mm x 5.5 mm. The distance between the

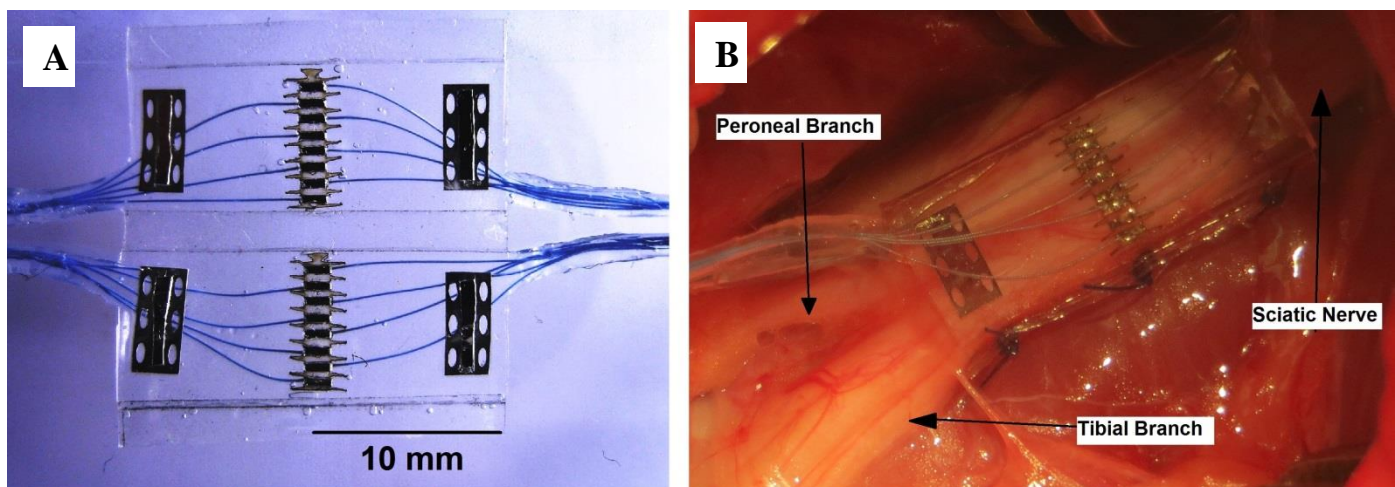


**Figure 3: FINE structure and implant site for neural activity recording.** **A)** The fabricated 16- contact FINE. The inner surface of the electrode is shown in the opened position. The other two free ends are sutured together to close the cuff around the nerve and the wires become parallel to the nerve as they exit near the spine of the electrode. **B)** FINE placement around the sciatic nerve relative to the branching point. The center contacts are evenly distributed across the main trunk to record from different segments within the nerve, thus allowing selective recording from the two functional groups inside the sciatic nerve before branching off to the two main targeted muscles.

1 references on the same side was 18 mm center-to-center, and the total electrode length was 21 mm.  
2  
3  
4  
5

### 6 *E. in-vivo* Neural Activity Recording 7

8 To test the constructed amplifier for physiological nerve activity recording, a FINE was  
9 implanted on the sciatic nerve of a mongrel-hound dog under chronic preparation (Fig. 3B). The neural  
10 activity of the sciatic nerve was recorded while the dog is walking on a treadmill. The movement of the  
11 ankle joint was simultaneously recorded with an optical tracking system (OptiTrack™, NaturalPoint,  
12 Inc.). These recordings were conducted three weeks post implant. The protocol for these experiments  
13 was approved by the Case Western Reserve University IACUC and the U.S. Army Medical Department  
14 ACURO.  
15  
16  
17  
18  
19  
20  
21  
22  
23

## 24 III. RESULTS 25

### 26 A) Input referred noise reduction by hardware averaging depends on source resistance values 27

28 Equation 1 indicates that hardware averaging reduces the amplifier-induced voltage noise ( $e_n$   
29 and  $\frac{e_{no}}{G}$  terms) by a factor of  $\sqrt{N}$  but does not affect the thermal noise generated by the sources. The  
30 current noise contribution is cumulative and increasing with the addition of more parallel devices,  
31 therefore the reduction in the total noise ( $V_n$ ) equals to  $\sqrt{N}$  only if the source resistance is zero.  
32  
33

34 For a non-zero source resistance, the thermal noise of the source and the amplifier's cumulative  
35 current-noise contribution are not reduced by averaging because their observed values are not random  
36 and do not vary among the parallel devices.  
37  
38

39 The current noise of the selected CMOS OTA was measured as described in the method section and  
40 found to be  $50 \text{ fA}/\sqrt{\text{Hz}}$ . The contribution of this low current-noise is not significant in comparison to the  
41 other factors for FINE source resistance range ( $0.5 \text{ nV}/\sqrt{\text{Hz}}$  at  $R_s=10\text{k}$ , comparing to  $e_n$  of  $20 \text{ nV}/\sqrt{\text{Hz}}$   
42 and  $e_T$  of  $13 \text{ nV}/\sqrt{\text{Hz}}$  ).  
43  
44  
45  
46  
47  
48  
49  
50  
51  
52  
53  
54  
55  
56  
57  
58  
59  
60

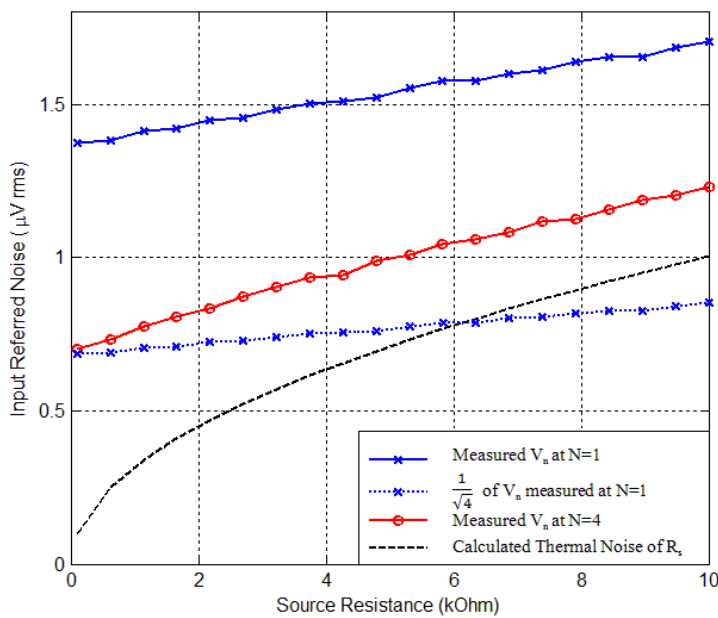


**Figure 4: Effect of source impedance on hardware averaging improvement.** The total input referred noise was measured for single and 4 parallel OTAs and a  $\sqrt{N}$  reduction from the single OTA was computed. Hardware averaging only reduces the intrinsic voltage noise term ( $V_n$ ) as a result the noise reduction is less than  $\sqrt{N}$  for high source resistance. Source induced noise determine the lower boundary for  $V_n$ .

To determine the influence of source resistance value on hardware averaging,  $V_n$  was measured for a single CMOS OTA ( $N=1$ ) and parallel CMOS OTAs configuration ( $N=4$ ) throughout 10k $\Omega$  source resistance range, and then reduction in the observed  $V_n$  at  $N=1$  was computed for comparison with the expected reduction without a source (Figure 4).

For very small  $R_s$ , the noise reduction can be approximated to a  $\sqrt{N}$  ( $R_s=100\Omega$  in Fig.4). For higher source resistances, the source-induced thermal noise becomes more significant factor in determining  $V_n$  and unlike the intrinsic voltage noise contribution of the parallel OTAs, it is not reduced by averaging and reduces the effect on the total  $V_n$ . This effect is represented by the increasing divergence between  $V_n$  at  $N=4$ , and the  $\sqrt{4}$  reduction to the original  $V_n$  at  $N=1$  for higher  $R_s$  values.

Although the previous results show a decreased proportion of noise reduction for higher source resistances, the resulting improvement is significant across the tested range. Hardware averaging reduces  $V_n$  closer to the thermal noise of the source itself which represents the lower boundary for  $V_n$ , and can be beneficial for cuff recording as it decreased the total noise to less than  $1\mu\text{V}_{\text{RMS}}$  in the presence of 4k $\Omega$  source.

### B) Cuff recording of physiological neural activity in chronic preparation

To study the efficacy of the parallel amplifier design during chronic recordings, and to determine if the intrinsic noise of the acquisition device is a significant factor in  $V_n$ , the neural activity of the sciatic nerve of dog was recorded with a 16-contact FINE during voluntary walking in a chronic preparation.

Simultaneous measurements of the ankle joint movement were obtained along with the neural activity recording. Each FINE contact was connected to 8 parallel CMOS OTAs. The output of each of these OTAs was recorded simultaneously (total of 128) and then the recorded outputs were averaged in groups of 1 through 8 per contact for comparison.

Fig. 5 shows the effect of averaging on the recorded activity in the time domain for 4 contacts equally positioned around the nerve. With  $N=1$ , the intrinsic noise of a single CMOS OTA is quite large and completely masks the neural activity. However, the intrinsic noise contribution of the parallel OTAs ( $N=4$  and 8) are significantly reduced by hardware averaging thereby uncovering the underlying low

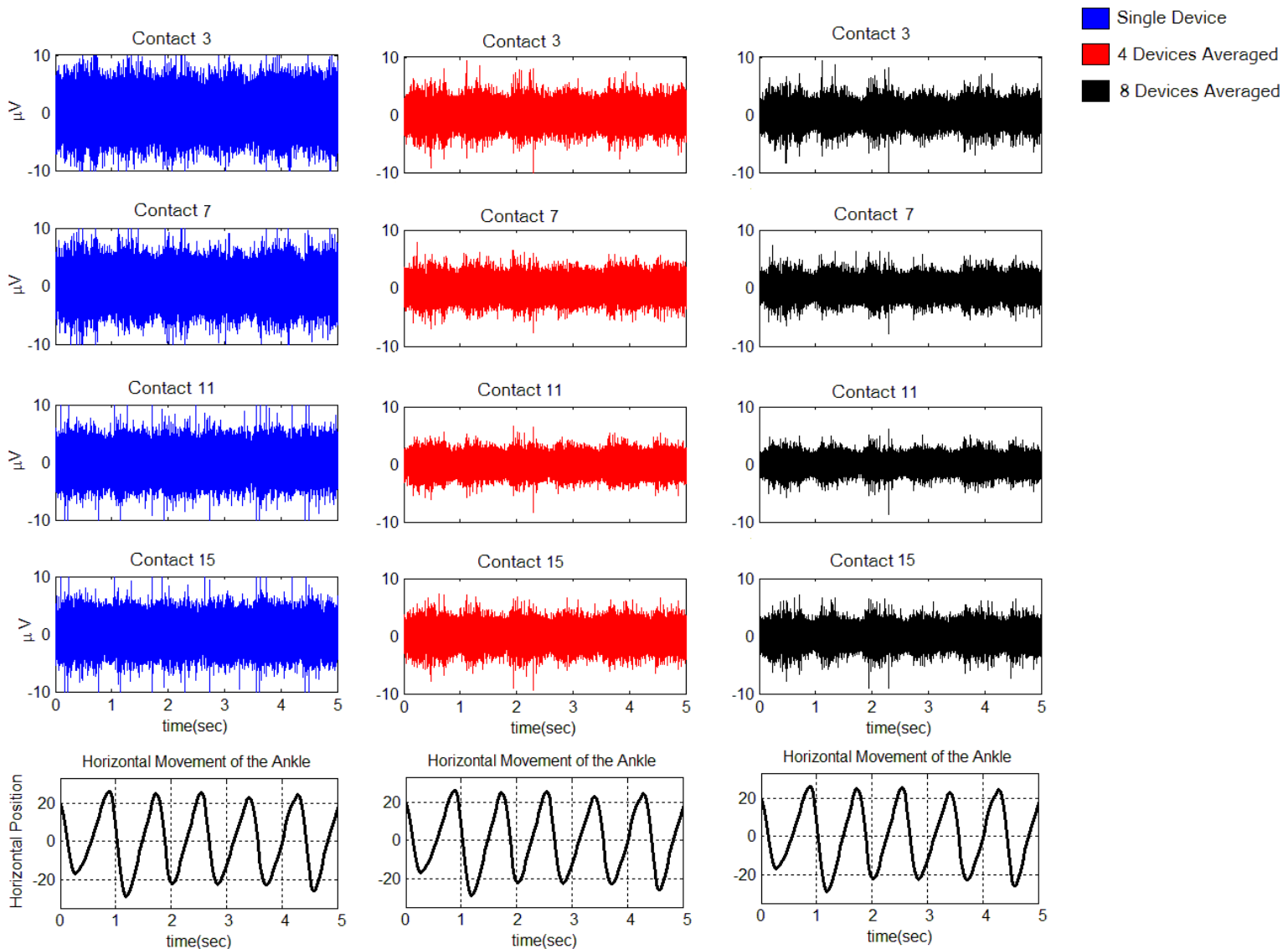


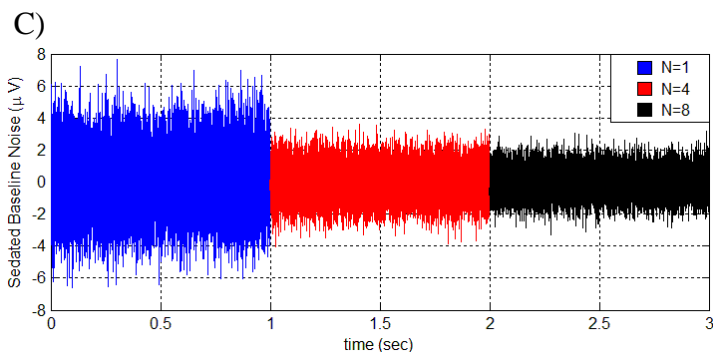
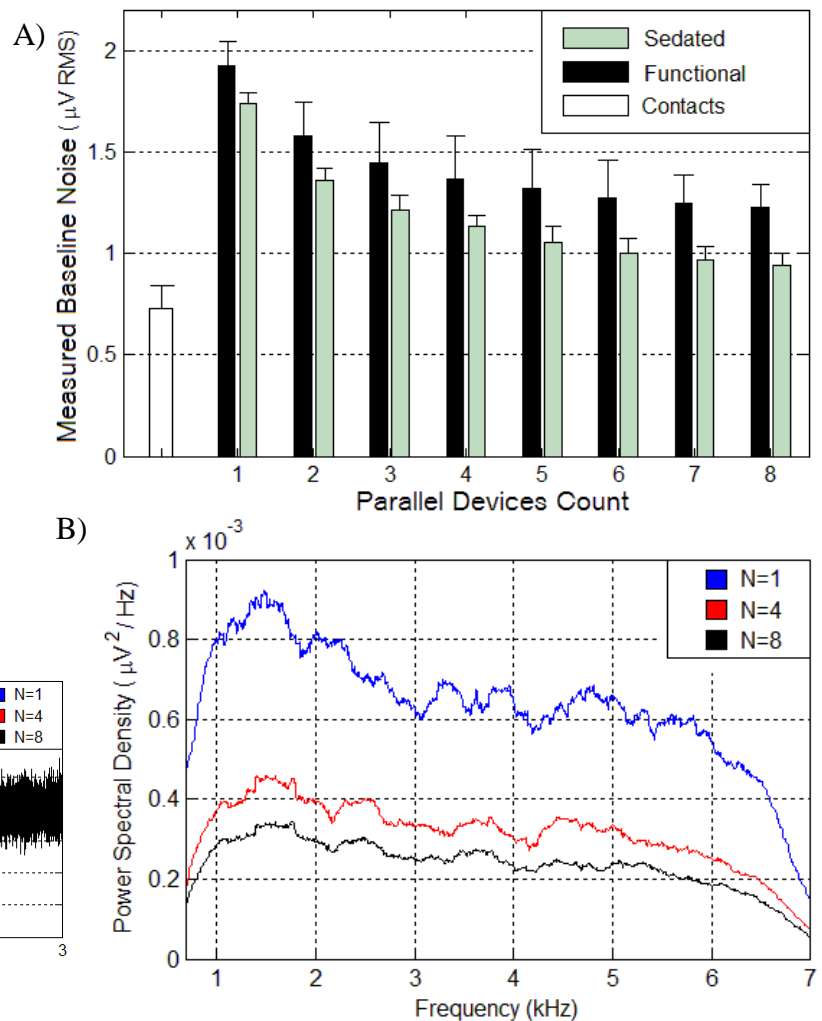
**Figure 5: Hardware averaging recording obtained 4-week post-implantation in a chronic dog. A)** Up to 8 parallel devices per contacts were used to record the neural activity of the sciatic nerve in dog while walking on treadmill. The outputs of a single, four and 8 parallel OTA devices are shown for the same time segment. The corresponding movement of the ankle was measured and plotted to compare the movement outcome to the recorded activity.

magnitude neural activity. The ankle movement is synchronized with the alternating ENG activity profile during rhythmic movement of the ankle during walking.

A parameter of interest in quantifying this effect is baseline noise reduction. It was defined under three conditions. The “*contact*” baseline is the noise level calculated as Johnson noise alone for each contact. The “*sedated*” baseline is obtained while the animal is sedated and lying down. This noise includes contact noise as well as intrinsic amplifier noise and low level neural activity. The “*functional*” baseline is obtained with the animal standing still on the treadmill and includes additional neural activity related to maintaining standing position.

As the number of parallel amplifiers is increased, both the functional and sedated noise levels are decreased significantly towards the lowest possible limit indicated by the contact noise value of  $0.69 \pm 0.13 \mu V_{RMS}$  (Fig.6A). The sedated baseline reduction (46.1%) is more pronounced compared to the functional baseline noise reduction (36.2%) at N=8 due to the fact that the sedated baseline includes a larger portion of the amplifier intrinsic noise. The sedated baseline noise at N=8 is  $0.93 \pm 0.06 \mu V_{RMS}$

**Figure 6: The effect of hardware averaging on recorded neural activity.** **A)** “Sedated” and “functional” baseline noise levels improve with increasing number of amplifiers in parallel compared to the noise of a single “contact” measured at 1 kHz). **B)** Power spectral density of a 10 second segment of the “sedated” baseline for N=1,4 and 8. **C)** One second segment of the “sedated” baseline recorded from the same contact. B and C shows that the improvement is more pronounced for higher values of N.



which is only  $0.2 \mu\text{V}_{\text{RMS}}$  above the lowest possible noise generated by the contacts indicating that this new amplifier design contributes little to the total noise. One-way ANOVA with post-hoc t-tests on the functional baseline showed significant improvement between  $N=1$  and  $N=2$  ( $P = 0.008$ ). Further reduction by increasing  $N$  beyond 2 was not statistically significant until  $N=6$  ( $P = 0.015$ ).

Another parameter of interest in cuff recordings is the SNR. To determine the impact of hardware averaging on this parameter we introduced the functional SNR (fSNR) to reflect the dynamic range of activity that is generated during walking. fSNR is defined as the ratio of the highest and lowest activity levels for each gate cycle, then the mean ratio was obtained over 50 gate cycles (Fig.7A).

Fig.7B shows that values fSNR increases as the amplifier count is increased. One-way ANOVA with post-hoc t-tests showed the first significant improvement at  $N=3$  ( $P = 0.01$ ). Further improvement by increasing  $N$  beyond 3 was not statistically significant until  $N=7$  ( $P = 0.04$ ).

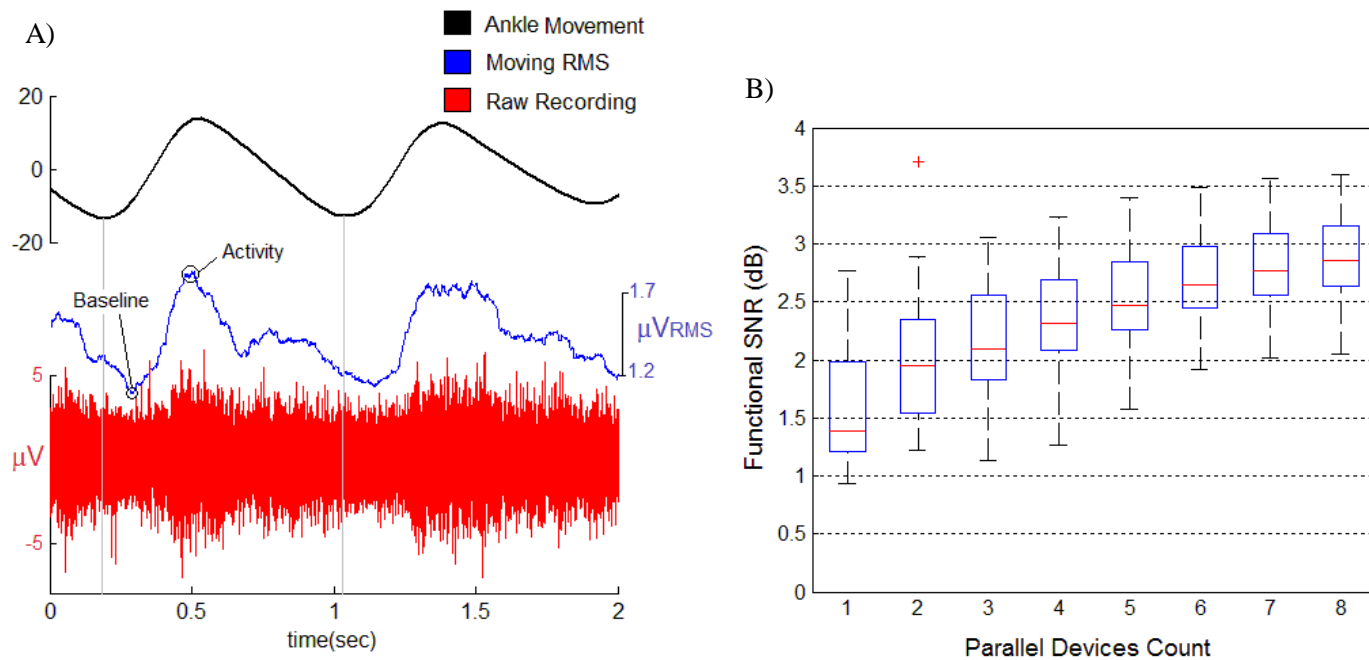


**Figure 7: Functional SNR.** A) The local maxima and minima of the rectified recording within each gate cycle were traced at  $N=8$  to measure the functional SNR, then the time stamp for these points were repeated among all other  $N$  count. B) The effect of averaging on the fSNR. The central mark is the median, the edges of the box are the 25th and 75th percentiles, and the whiskers extend to the most extreme data points not considered outliers.

C) Optimization of the number of parallel devices

The minimum for  $V_n$  from Equation (1) can be obtained and yields a unique value equal to:

$$N_{\text{Minimum}} = \frac{e_n}{i_n |Z_{we}|} \quad (\text{for } |Z_{we}| \gg |Z_{re}|) \quad (3)$$

For the RHA2132,  $N_{\text{Minimum}} = 87$ . This large number of amplifiers increases the power consumption significantly and this approach in choosing N is not practical. Here we seek to determine an optimum value of N for given amplifier design that will minimize both noise and power for a given source. The noise efficiency factor (NEF) is normally used to quantify power consumption for a given noise level [22, 23]. For N devices in parallel, its value is given:

$$\text{NEF} = \sqrt{\frac{(N \cdot e_{T(we)}^2 + e_n^2 + N^2 i_n^2 |Z_{we}|^2) \cdot 2 \cdot I_o}{\pi \cdot U_T \cdot 4kT \cdot BW}} \quad (4)$$

where  $I_o$  is the total supply current for a single device,  $U_T$  is the thermal voltage, BW is the bandwidth of interest, T is the absolute temperature, and k is Boltzmann's constant

A plot of both the relative NEF and  $V_n$  as a function of N (Figure 8A) shows that the relative NEF increases while  $V_n$  decreases with increasing the value of N. Therefore, an optimization algorithm is needed to obtain a value of N to minimize both NEF and  $V_n$  simultaneously. This is known as a multivariate optimization problem that can be solved by minimizing the following objective function:

$$E = W_1 \cdot \left( \frac{V_{nN} - V_{nmin}}{V_{n(N=1)}} \right)^2 + W_2 \cdot \left( \frac{NEF_N - NEF_{min}}{NEF_{(N=1)}} \right)^2 \quad (5)$$

where  $W_1, W_2$  are the weights for each variable.

There is a unique value of N to minimize E for each

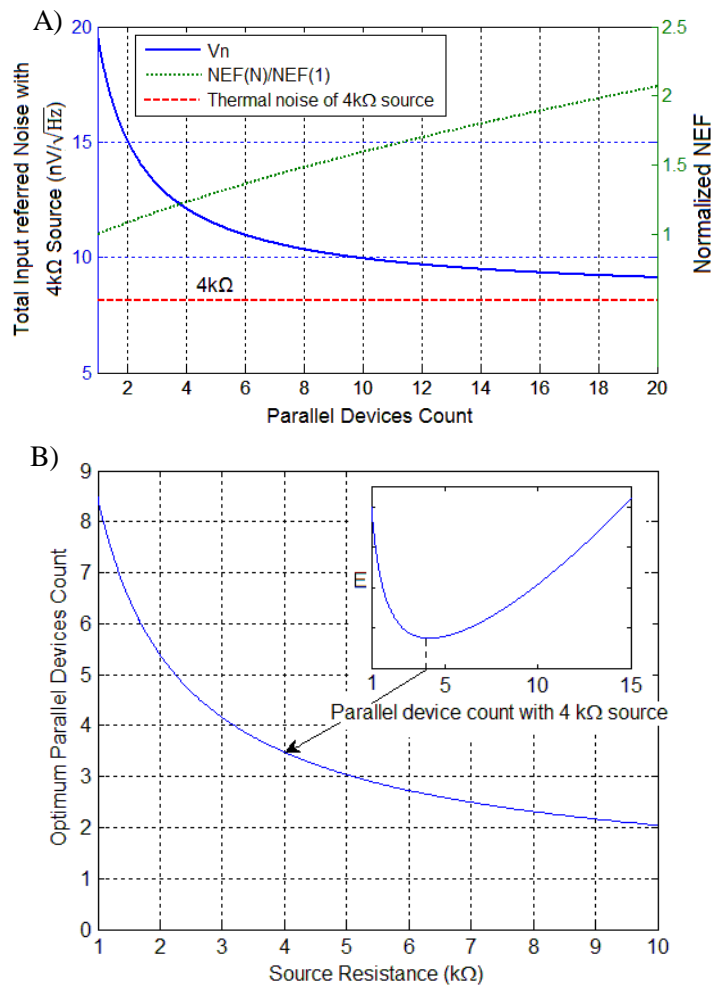


**Figure 8: Parallel devices optimization for RHA2132 chip.** A) Effect of increasing N on the total input referred noise and the normalized NEF. An optimization approach is applied for to determine the optimal number of amplifiers. B) Optimum value of N vs source resistance. For each source resistance value, optimum N minimizes the parameter E that represents the voltage noise reduction with respect to cost of NEF degradation. An insert shows that that a value of N=3.5 is optimum (minimizes E) for  $R_s = 4k\Omega$ .

value of  $R_s$ . These optimal  $N$  values were calculated and plotted in Fig 8B. As the value of  $R_s$  increases, the optimum value of  $N$  decreases and a lower count of parallel devices is needed to get the most power efficient amplifier design for a given noise level. Different weights can be assigned to give more emphasis on either the power efficiency or noise reduction.

Applying this optimization method to the 32-channel RHA2132 with equal weights assigned to power and noise ( $W_1/W_2=1$ ) yields an optimum  $N$  of 4. Changing the weights to emphasize noise reduction over power consumption ( $W_1/W_2=4$ ) to the 64-channel RHD2164 yields an optimum  $N$  of 8. As a result, two 16-ch low-noise amplifiers were built using these two options and the measurements reflect a decrease in noise for  $N=8$  but also an increase in power (see Table 1).

RHD2164 showed higher noise level than the RHA2132 chip (up to 20%) and most of that extra noise was spot noise observed at 5kHz. However, the advantage of using this chip is that only 10 interface lines are needed since it has a built-in A/D converter, and the digital LVDS output format provides superior noise-immunity. Also it is available in  $7.3 \times 4.2 \times 0.2 \text{ mm}^3$  bare-die form. These features make this option a favourable choice for implantable neural recording applications.

Option	Chip	$W_1/W_2$	$N_{\text{optimum}}$	Measured Noise ( $R_s=4\text{k}\Omega$ , 700Hz-7kHz)		Power/Channel (3.3V supply)
				700Hz-5kHz	700Hz-7kHz	
1	RHA2132	1	4	$0.77 \pm 0.02 \mu\text{VRMS}$	$0.90 \pm 0.03 \mu\text{VRMS}$	1.63 mW/ch
2	RHD2164	4	8	$0.68 \pm 0.02 \mu\text{VRMS}$	$0.79 \pm 0.04 \mu\text{VRMS}$	4.6 mW/ch

**Table 1:** Noise measurement and power consumption for 16-channel ultra-low noise amplifiers based on RHA and RHD series chips. Different noise and power emphasis was used by changing  $W_1/W_2$  in equation 5. Note that the  $4\text{k}\Omega$  source by itself generates  $0.6 \mu\text{VRMS}$  thermal noise, which is included in these noise measurements.

#### IV. DISCUSSION AND CONCLUSION

Hardware averaging can provide a practical approach to ultra-low noise amplification for neural recording with high source resistance cuff electrodes. This approach improves the noise performance of existing acquisition devices and an alternative of implementing a customized ASIC design flow for similar applications. The noise levels achieved with this design are comparable to those obtained using

1  
2 either an input transformer [11, 16, 18, 29, 31], or a low, voltage-noise solid state amplifier [24, 28] for  
3  
4 single-channel whole nerve recording and contact impedances less than 1Kohm.

5  
6 The noise reduction effect of hardware averaging at the acquisition system side is prominent for  
7  
8 lower source impedance values (Fig.4) where it can be approximated to a  $\sqrt{N}$  reduction. As  $R_s$  is  
9  
10 increased, the source-induced noise ( $V_n$ ) becomes the dominating factor, and since the source-induced  
11  
12 noise is not random among the parallel OTAs, it is not reduced with averaging leading to a reduction of  
13  
14 less than  $\sqrt{N}$  in the presence of high source values.

15  
16  
17 The selected OTA has low input current noise ( $50 \text{ fA}/\sqrt{\text{Hz}}$ ). This criterion is essential in choosing  
18  
19 the device for hardware averaging with high source impedance. High current-noise devices (BJT input  
20  
21 amplifiers in particular) will rapidly shift the resulted  $V_n$  away from a  $\sqrt{N}$  reduction and can even  
22  
23 degrade the noise performance if the cumulative current noise effect exceeds the original intrinsic  
24  
25 voltage noise. As a result, these devices can benefit from averaging only if  $R_s$  is very small and should  
26  
27 be avoided for high source applications.

28  
29  
30 Connecting one amplifier per contact then averaging the outputs of several of these electrode-  
31  
32 amplifier units will result in a full  $\sqrt{N}$  reduction regardless of the source impedance value as reported in  
33  
34 [27, 32, 33] since the source-induced noise is random among these units and all the terms of  $V_n$  will be  
35  
36 reduced by the same proportion. This scenario can be applied to multiple contact cuff recording by  
37  
38 averaging the recordings from multiple adjacent contacts. Although spatial resolution of these  
39  
40 recordings will be degraded, it can be useful for whole nerve recording or selective recording from small  
41  
42 numbers of neural sources.

43  
44  
45 The implemented multi-channel amplifier was used to record physiological neural activity from dog  
46  
47 sciatic nerve under chronic preparation. Reducing the intrinsic voltage noise of the amplifier was  
48  
49 sufficient and could reveal neural signals that were originally below baseline noise level with a single  
50  
51 OTA (Fig. 5). Both types of baseline noise (functional and sedated) were reduced significantly and the  
52  
53 majority of the recorded noise at  $N=8$  was induced by the source (Fig. 6A).

54  
55  
56 The functional SNR was defined as the ratio of maximum and minimum activity during each  
57  
58 gate to represent the usable range of nerve activity that is primarily produced during walking. A  
59  
60

1 significant improvement in the fSNR was observed with increasing N. The recorded neural signals can  
2 be processed further with spatial filtering algorithm (i.e. beam forming algorithm [13]) to create an  
3 image estimating the source activity in the nerve's cross section. The accuracy of these estimations  
4 depends on the SNR of the recorded activity to uncover the underlying activity detected by each  
5 contact.  
6  
7  
8  
9  
10  
11

12 The impact of hardware averaging is predominant for lower number of parallel devices, and  
13 becomes less significant among higher values of N. Therefore, arbitrarily increasing N to target the  
14 lowest possible  $V_n$  is not practical and the improvement will not justify the required increase in power  
15 consumption. Therefore, a cost function was introduced (E in equation 5) to balance these two factors.  
16 Equal weights were assigned to the power consumption and the noise. Minimizing E (Fig. 8B) could  
17 provide a unique N for a given source impedance value.  
18  
19  
20  
21  
22  
23  
24  
25  
26  
27

28 **Acknowledgments:** I would like to thank Dr. Brian Wodlinger for his ideas and assistance in this study,  
29 Andrew Czarnecki and Dr. Bryan L. McLaughlin from Draper Laboratory for the assembly of 16ch  
30 amplifier with N=8 averaging, and William Marcus for his assistance in animal care, the implant  
31 operation, and chronic recording. This work was sponsored by the Defence Advanced Research  
32 Projects Agency (DARPA) MTO under the auspices of Dr. Jack Judy and Dr. Doug Weber through the  
33 Space and Naval Warfare Systems Center, Pacific Grant/Contract No.N66001-12-C-4173.  
34  
35  
36  
37  
38  
39  
40  
41  
42

### 43 References

- 44  
45  
46 [1] Kristoffer Famm, Brian Litt, Kevin J. Tracey, Edward S. Boyden & Moncef Slaoui *Charged by GSK investment,*  
47 *"battery of electroceuticals advance"., Nature 496,159–161 (11 April 2013)*  
48  
49 [2] Branner, Almut, et al. "Long-term stimulation and recording with a penetrating microelectrode array in cat  
50 sciatic nerve." *Biomedical Engineering, IEEE Transactions on* 51.1 (2004): 146-157.  
51  
52 [3] Kuiken, Todd A., et al. "Targeted muscle reinnervation for real-time myoelectric control of multifunction artificial  
53 arms." *Jama* 301.6 (2009): 619-628.  
54  
55 [4] Micera, Silvestro, et al. "On the use of longitudinal intrafascicular peripheral interfaces for the control of  
56 cybernetic hand prostheses in amputees." *Neural Systems and Rehabilitation Engineering, IEEE Transactions on*  
57 16.5 (2008): 453-472.  
58  
59  
60

- 1  
2 [5] Tyler, Dustin J., and Dominique M. Durand. "A slowly penetrating interfascicular nerve electrode for selective  
3 activation of peripheral nerves." *Rehabilitation Engineering, IEEE Transactions on* 5.1 (1997): 51-61.  
4
- 5 [6] Rossini, Paolo M., et al. "Double nerve intraneural interface implant on a human amputee for robotic hand  
6 control." *Clinical neurophysiology* 121.5 (2010): 777-783.  
7
- 8 [7] Branner, Almut, and Richard Alan Normann. "A multielectrode array for intrafascicular recording and  
9 stimulation in sciatic nerve of cats." *Brain research bulletin* 51.4 (2000): 293-306.  
10
- 11 [8] Navarro, Xavier, et al. "A critical review of interfaces with the peripheral nervous system for the control of  
12 neuroprostheses and hybrid bionic systems." *Journal of the Peripheral Nervous System* 10.3 (2005): 229-258.  
13
- 14 [9] Tyler, Dustin J., and Dominique M. Durand. "Functionally selective peripheral nerve stimulation with a flat  
15 interface nerve electrode." *Neural Systems and Rehabilitation Engineering, IEEE Transactions on* 10.4 (2002):  
16 294-303.  
17
- 18 [10] Wodlinger, B., and D. M. Durand. "Peripheral nerve signal recording and processing for artificial limb control."  
19 *Engineering in Medicine and Biology Society (EMBC), 2010 Annual International Conference of the IEEE.* IEEE,  
20 2010.  
21
- 22 [11] Sahin, Mesut, et al. "Spiral nerve cuff electrode for recordings of respiratory output." *Journal of Applied*  
23 *Physiology* 83.1 (1997): 317-322.  
24
- 25 [12] Andersen, Mads P., et al. "Chronic cuff electrode recordings from walking Göttingen mini-pigs." *Engineering*  
26 *in Medicine and Biology Society, EMBC, 2011 Annual International Conference of the IEEE.* IEEE, 2011.  
27
- 28 [13] Durand, D.M, Park, H.J. ; Wodlinger, B. "Localization and control of activity in peripheral nerves", *Engineering*  
29 *in Medicine and Biology Society*, 2008.  
30
- 31 [14] Hassibi, Arjang, et al. "Comprehensive study of noise processes in electrode electrolyte interfaces." *Journal*  
32 *of applied physics* 96.2 (2004): 1074-1082.  
33
- 34 [15] Gondran, C., et al. "Noise of surface bio-potential electrodes based on NASICON ceramic and Ag- AgCl." *Medical and Biological Engineering and Computing* 34.6 (1996): 460-466.  
35
- 36 [16] Sahin, Mesut. "A low-noise preamplifier for nerve cuff electrodes." *Neural Systems and Rehabilitation*  
37 *Engineering, IEEE Transactions on* 13.4 (2005): 561-565.  
38
- 39 [17] J O Lekkala and J A Malmivuo, "Noise Reduction Using a Matching Input Transformer", *J. Phys, E. Sci.*  
40 *Instrum.*, Vol. 14, 1981.  
41
- 42 [18] Sahin, Mesut, Dominique M. Durand, and Musa A. Haxhiu. "Chronic recordings of hypoglossal nerve activity  
43 in a dog model of upper airway obstruction." *Journal of Applied Physiology* 87.6 (1999): 2197-2206.  
44
- 45 [19] Poussart, Denis J-M. "Low-Level Average Power Measurements: Noise Figure Improvements Through  
46 Parallel or Series Connection of Noisy Amplifiers." *Review of Scientific Instruments* 44.8 (2003): 1049-1052.  
47
- 48 [20] Barach, JOHN PAUL, Bradley J. Roth, and John P. Wiksw. "Magnetic measurements of action currents in a  
49 single nerve axon: A core-conductor model." *Biomedical Engineering, IEEE Transactions on* 2 (1985): 136-140.  
50
- 51 [21] Leach Jr, W. Marshall. "Fundamentals of low-noise analog circuit design." *Proceedings of the IEEE* 82.10  
52 (1994): 1515-1538.  
53
- 54 [22] Harrison, Reid R., and Cameron Charles. "A low-power low-noise CMOS amplifier for neural recording  
55 applications." *Solid-State Circuits, IEEE Journal of* 38.6 (2003): 958-965.  
56
- 57 [23] Steyaert, Michel SJ, Willy MC Sansen, and Chang Zhongyuan. "A micropower low-noise monolithic  
58 instrumentation amplifier for medical purposes." *IEEE journal of solid-state circuits* 22.6 (1987): 1163-1168.  
59  
60

- 1  
2 [24] Lin, Chou-Ching K., Ming-Shaung Ju, and Hang-Shing Cheng. "Model-based ankle joint angle tracing by cuff  
3 electrode recordings of peroneal and tibial nerves." *Medical & biological engineering & computing* 45.4 (2007):  
4 375-385.
- 5  
6 [25] Triantis, I. F., A. Demosthenous, and N. Donaldson. "Comparison of three ENG tripolar cuff recording  
7 configurations." *Neural Engineering, 2003. Conference Proceedings. First International IEEE EMBS Conference*  
8 *on. IEEE*, 2003.
- 9  
10 [26] Brinkman, K. "Analysis of noise with the use of electrodes on the skin surface", Master's thesis, Delft  
11 Technical University, 1993.
- 12  
13 [27] N. Donaldson, R. Rieger, M. Schuettler, J. Taylor, "Noise and Selectivity of Velocity-Selective Multi-Electrode Nerve  
14 Cuffs," *Medical & Biological Engineering & Computing*, no. 46, pp. 1005-1018, 2008
- 15  
16 [28] Haugland, Morten K., and Thomas Sinkjaer. "Cutaneous whole nerve recordings used for correction of  
17 footdrop in hemiplegic man." *Rehabilitation Engineering, IEEE Transactions on* 3.4 (1995): 307-317.
- 18  
19 [29] Loeb, G. E., and R. A. Peck. "Cuff electrodes for chronic stimulation and recording of peripheral nerve  
20 activity." *Journal of neuroscience methods* 64.1 (1996): 95-103.
- 21  
22 [30] Rahal, R, et al. "An improved configuration for the reduction of the EMG in electrode cuff recordings." *IEEE Trans.*  
23 *Biomed. Eng.*, 74, (2000) pp. 565-568.
- 24  
25 [31] Nikolic, Zoran M., et al. "*Instrumentation for ENG and EMG recordings in FES systems.*" *Biomedical*  
26 *Engineering, IEEE Transactions on* 41.7 (1994): 703-706.
- 27  
28 [32] Rieger, R, Taylor, J, "Design strategies for multi-channel low-noise recording systems", *Analog Integrated Circuits*  
29 *and Signal Processing*, 58 (2009), pp123-132.
- 30  
31 [33] Taylor, J, et al. "Multiple-electrode nerve cuffs for low velocity and velocity-selective neural recording", *Medical and*  
32 *Biological Engineering and Computing*, Vol 42, (2004), pp634-643.
- 33  
34 [34] Stein, Richard B., et al. "*Stable long-term recordings from cat peripheral nerves.*" *Brain research* 128.1  
35 (1977): 21-38.
- 36  
37 [35] Boretius, Tim, et al. "*A transverse intrafascicular multichannel electrode (TIME) to interface with the*  
38 *peripheral nerve.*" *Biosensors and Bioelectronics* 26.1 (2010): 62-69.  
39  
40  
41  
42  
43  
44  
45  
46  
47  
48  
49  
50  
51  
52  
53  
54  
55  
56  
57  
58  
59  
60